Article

The Role of Empirical Formulae in the Design of Complex Systems

Alessandro Curcio, Giuseppe Dattoli and Emanuele Di Palma

Article

The Role of Empirical Formulae in the Design of Complex Systems

Alessandro Curcio [1], **Giuseppe Dattoli** [2,*] **and Emanuele Di Palma** [2]

1 Centro de Laseres Pulsados (CLPU), Edificio M5, Parque Científico, C/Adaja, 8, 37185 Villamayor, Spain
2 ENEA Frascati Research Center, Via Enrico Fermi 45, 00044 Rome, Italy
* Correspondence: pinodattoli@libero.it

Abstract: We discuss the general concepts underlying the design strategies of complex devices like Tokamaks and Free Electron Lasers (FEL). Regarding the FEL, starting from the desired output performances, the key parameters are embedded to get a set of semi-analytical/empirical equations yielding straightforward and reliable estimates of gain and power. In a similar way, the guiding elements of a fusion reactor, to reach the prescribed fusion gain Q and power, are defined in terms of scaling relations involving pivotal quantities like radius and magnetic field. General formulae characterizing a physical system may be the consequence of an unknown symmetry. The onset of specific instabilities represent the breaking of a symmetry characterizing given equilibrium conditions. In this article, we comment on the analogy between two different physical devices, and even though we do not specify any underlying symmetry, we aim to stimulate further research in this direction.

Keywords: empirical formulae; complex systems; instabilities

1. Introduction

This article is written for a composite audience, namely for experts of Free Electron Laser (FEL) devices and for experts of magnetic fusion and Tokamak design. Since the overlapping expertise between the two disciplines is not necessarily tight, we keep the forthcoming discussion on general grounds, by underscoring the elements of common interest, which may illustrate analogies between fields of research that are seemingly far from each other [1]. The most obvious element of contact is that either the FEL [2] or Tokamak [3] aim at transforming energy of one kind into another. FELs "capture" power from a relativistic e-beam to convert it into laser-like radiation, while Tokamaks convert nuclear potential into heat power. Otherwise, they are completely different devices, having, as common elements, the complexity of their constitutive elements. The relevant design criteria are aimed at dimensioning the relevant pivotal parameters to maximize, in both systems, the power amplification factor. This quantity, when associated with FELs or Tokamaks, has different meanings. To better specify the framework in which we are moving, we remind readers that FELs are devices producing laser light by converting the power of a relativistic electron beam into coherent electromagnetic power. The gain is accordingly defined as for conventional laser systems and specifies the fractional increase of the field intensity per unit length. In the case of Tokamaks, which aim to produce power from a fusion process, the gain, or better the Q amplification factor, is the ratio

$$Q = \frac{P_{fus}}{P_{heat}},$$ (1)

where the numerator is the power obtained through the process of fusion itself and the denominator is the total heating power (including the Ohmic contribution and the auxiliary

power) employed to reach the break-even point. In FEL devices, the laser output power is given by the ratio

$$\rho = \frac{P_{fel}}{P_b},$$ (2)

where P_b is the electron beam power and ρ, known as the Pierce parameter, embeds significant quantities defining the constitutive elements of the whole device. Both equations summarize, in two simple expressions, a long conceptual and experimental pathway which yields the key note to exploit either Q and ρ as the reference parameter, for the design of the devices themselves. Two pillars of synthetic reasoning can be exploited as paradigmatic examples of how the different constitutive elements of a complex device can be embedded to achieve far reaching conclusions. Regarding plasma and FEL physics, two key points of reasoning based on simple physics have been used to estimate the achievable output power. One of the milestones of the fusion plasma design criteria is the Lawson triple product criterion [4], which fixes the "ignition" conditions. In the physics of storage ring (SR) operating FELs, the Renieri-limit [5,6] determines the efficiency of power delivery from the electron beam to the laser field. Although arising in different physical contexts, the derivation of the previously quoted criteria proceeds from similar logical elaborations, as briefly described below. The power delivered in a fusion process is roughly given by the "wise" identity

$$P_{fus} = V n_D n_T E_{fus} \langle \Sigma \rangle$$ (3)

The first term V is the contained volume, n_D and n_T are number densities of Deuterium and Tritium (in the following we will use $n_D = n_T = n/2$), respectively, and E_{fus} is the energy released per fusion process ($\simeq$17.6 MeV) with the assumption that it will all contribute to the plasma heating. The reactivity, namely the quantity denoted by $\langle \Sigma \rangle$, accounts for the dependence of the power P_{fus} on the rate of the fusion events. It can accordingly be defined as the product of the cross section of the fusion processes times the velocity at which it occurs, namely

$$\langle \Sigma \rangle \simeq \sigma v$$ (4)

The next step is that of specifying the amount of fusion power lost (P_{loss}) to the environment, during the energy confinement time τ_E. The most natural mechanism is the heating of the surrounding plasma, therefore we can write (where T is the plasma temperature)

$$\frac{P_{loss}}{V} = \frac{3 n k_B T}{\tau_E}$$ (5)

Requiring that $P_{fus} > P_{loss}$, we end up with the condition (the numerical factors on the right-hand side are obtained by inserting typical values for the plasma temperature and reactivity)

$$n \tau_E > \frac{12 k_B T}{E_{fus} \langle \Sigma \rangle} \simeq 1.5 \times 10^{20} \frac{s}{m^3}$$ (6)

The previous equation states that the fulfillment of the break-even conditions require that the product of the plasma density and confinement time should exceed a certain threshold value.

Regarding the Renieri-limit, the reasoning follows an analogous conceptual strategy. In a free electron laser (see Figure 1), a beam of relativistic electrons moves inside a magnetic undulator, where it executes transverse oscillations and emits bremsstrahlung radiation. In a storage ring, the beam is recirculated many times through the undulator and the emitted radiation is stored and amplified inside an optical cavity [7]. The multiple electron–radiation interactions produce a "heating" of the beam, which determines the increase of its relative energy spread. This effect induces an interruption of the laser process and consequently stops the effects of heating. The associated energy loss by synchrotron radiation emission along the guiding magnets of the SR determines the cooling of the

e-beam, which restores the lasing conditions. In quantitative terms, the previous reasoning can be formulated as follows

a.   The relative energy spread induced by the interaction is $\langle \Delta E / E \rangle \simeq 1/2N$
b.   The RMS energy loss is accordingly $\langle \Delta E \rangle \simeq N_e E / 2N$, where N_e is the number of electrons inside the beam
c.   The cooling time is associated with the damping time, therefore the power radiated (P_s) in this process is

$$P_L \simeq \frac{\Delta E}{\tau_s} = \frac{P_s}{2N}$$

$$P_s = \frac{N_e E}{\tau_s} \tag{7}$$

which states that the laser power in a storage ring FEL process is a fraction of the power emitted via synchrotron radiation, inside the machine, during the damping time. Albeit describing different processes, it is evident that the essential elements of the reasoning are a balanced relationship with a characteristic time. In the forthcoming sections we will also discuss further the elements confirming the structural analogies in the design guidelines.
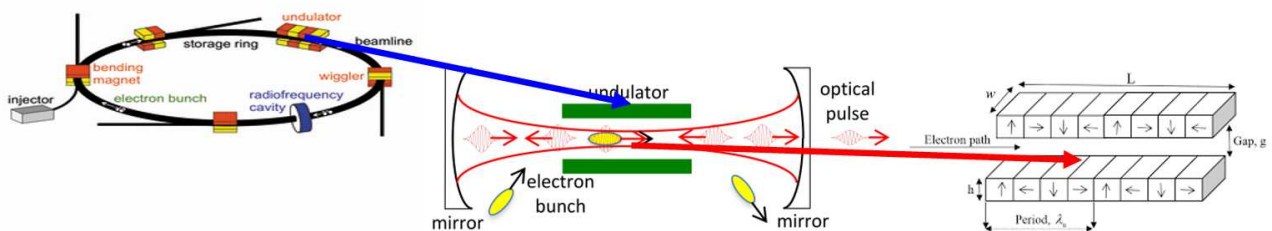

Figure 1. (**Left**) Storage ring layout: the circulating beam emits radiation inside the magnets, constituting the transport elements along the ring; (**Center**) In the case of an SR FEL, an optical cavity surrounds the undulator, where the emitted and amplified radiation is stored; (**Right**) Static field magnetic undulator: arrangement of north-south magnetic poles with a period λ_u and length $L = N\lambda_u$ with N total number of periods.

2. A Glimpse into the Design Strategies of Tokamaks

The design of a Tokamak fusion reactor is not a straightforward task, since it is constrained by plasma physics and engineering demands, which are not always aligned [8]. A sense of the complexity of the device can be gathered from Figure 2, which shows the constitutive elements of the device, including:

a   Geometrical, provided by the external (from the center of the Tokamak) radius and inner cross-sectional radius
b   Magnetic field elements concurring with the definition of the confining field
c   Plasma parameters: pressure, temperature, current, density, etc.

It would be desirable to fix the geometrical and electro-technical issues to determine the plasma conditions that could scale the Tokamak to an effective reactor, namely a Fusion Power Plant (FPP), i.e., a facility providing reliable and commercially convenient energy. Unfortunately, plasma physics imposes constraints on engineering and vice-versa. As already stressed in Ref. [8], a Tokamak designed on the basis of nuclear physics and standard engineering constraints does not scale to an FPP.
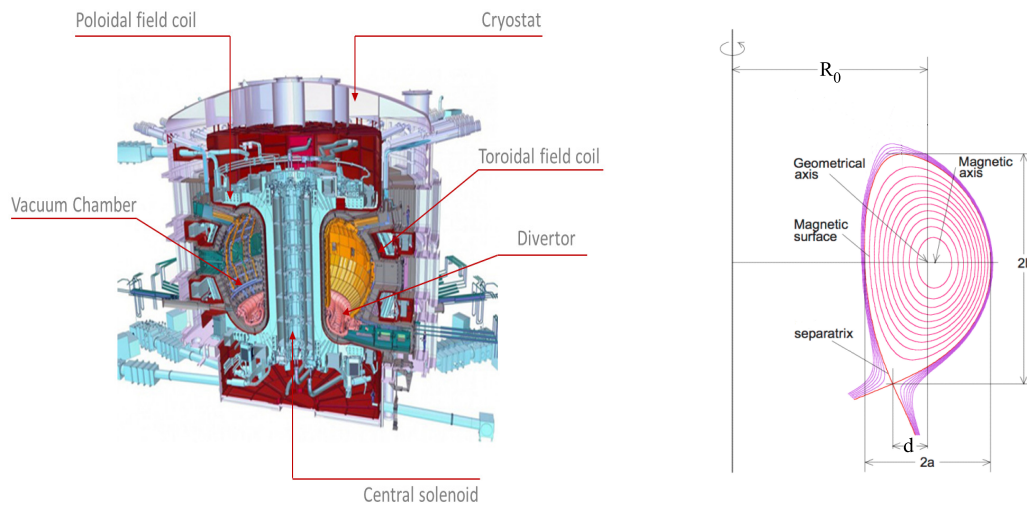
Figure 2. (**Left**) Cross section of a divertor in the Tokamak configuration with its principal elements; (**Right**) Plasma cross section shape of a divertor in the Tokamak configuration where the triangularity $\delta = d/a$, elongation $\kappa = b/a$, and aspect ratio $A = R_0/a$. Hence, the plasma volume can be estimated using the following expression: $V_p = (2\pi^2\kappa(A-\delta) + 16\pi\kappa\delta/3)a^3$.

The design of a Tokamak intended as a FPP, is based on the combination of "laws" derived from the extrapolation of theoretical ideas, the fitting of "laws" emerging from experimental campaigns on a specific machine, or resulting from massive numerical codes capable of embedding the various elements comprising a Tokamak [9,10]. Just to give an example, we note that fusion power can be written in terms of the quantities listed in the points (a)–(c) as in [11,12]

$$P_{fus}[MW] = C_{fus}\kappa\Lambda B^2 R_0^3, \qquad \Lambda = \kappa\frac{\beta_N B^2}{q^2 A^4} \tag{8a}$$

$$\beta_N = \frac{\beta}{A I_p / R_0 B}, \qquad \beta = \frac{p_p}{p_m}, \qquad p_m = \frac{B^2}{2\mu_0}, \qquad A = \frac{R_0}{a} \tag{8b}$$

where we have assumed that the triangularity $\delta = 0$ (see Figure 2), p_p is the kinetic plasma pressure, p_m is the pressure due to the magnetic field, A is the machine aspect ratio, I_p is the plasma current, q is the edge safety factor and C_{fus} is the combination of the physical constants in SI units. To ensure plasma stability, we satisfy the condition $q > 2$ [13]. The magnetic field is $\vec{B} = \vec{B}_t + \vec{B}_p$, where B_t is the thoroidal component and B_p the poloidal component. The messages contained in Equation (8a) are the manifolds. For example, it states that the fusion power scales with the total magnetic energy. It would accordingly suggest that a larger fusion power can be achieved in devices with larger magnetic field intensities and external radii. Clearly this imposes problems in terms of costs (if one is interested to commercialize the device) and also in terms of additional losses due to synchrotron radiation (P_{sync}) emission which, as reported in Refs. [13–15], behaves as

$$P_{sync} = 1.2 \times 10^{-7}(BT_{av})^{2.5}\sqrt{\frac{A}{R_0}}n_e\left(1 + \frac{18}{A\sqrt{T_{av}}}\right) \tag{9}$$

where T_{av} is the average plasma temperature, n_e is the electron density, and V is the plasma volume. If we use the ITER parameters $A = 3.1$, $q = 3.1$, $\beta_N = 1.8$, $B = 5.5$ T, and $R_0 = 6.8$ m we obtain a power around 400 MW.

According to the previous indications, the fusion power by itself is by no means enough to characterize a Tokamak reactor, as long as the corresponding Q factor is not specified. The evaluation of this quantity requires a scaling relationship analogous to that

for the fusion power. The physical respects of the associated engineering parameters as they pertain to the aforementioned scaling is worth stressing. It is indeed noted that the amplification factor exhibits the following qualitative behavior [16]

$$Q \propto \frac{1}{(BR_0)^{0.3}B^{-2}R_0^{-3} - c} = \frac{1}{B^{-1.7}R_0^{-2.7} - c} \tag{10}$$

where c is a constant. The non-integer exponents in Equation (10) come from the fitting of numerical/experimental data (see Refs. [11–13]). By means of Equation (9), we rewrite Equation (10) as

$$Q \propto \frac{1}{(BR_0)^{0.3}\Lambda P_{fus}^{-1} - c} \tag{11}$$

We can therefore consider a parameter configuration in which BR_0 is fixed and either B or R_0 are varied in order to fix the amplification factor at a convenient value that corresponds with the given value for the fusion power. In this section, we have just scraped the surface of an extensive field of research. In the forthcoming sections, we present an analogous discussion regarding the design of FEL devices.

3. Design Strategies for FEL Devices

In the previous section we have omitted any reference to dimensionless quantities characterizing a hot plasma. Going back to the 1970s, Kadomtsev proposed non-dimensional parameters [16], which are still currently used [17]. These quantities, derived through the Buckingham theorem (see ref. [18] for specific applications in engineering and physics), specify the already mentioned ratio (see Equation (8b)), the normalized Larmor radius ρ^*, and ν^*, which is associated with the connection length and the particle mean free path. They provide us with a well-defined reference quantity set for the design of a Tokamak device and almost all the plasma scaling relations can be expressed in terms of the triple (ρ^*, ν^*, β) [13–16].

In FEL devices employing long undulators and operating with electron bunches provided by high energy linacs, the laser field grows after undergoing different evolution steps reported in Figure 3 (see Figure caption for further details). The growth of the laser signal is determined by the first phase associated with the energy modulation, then bunching and linear growth induces an increase of the electron energy spread, which eventually leads to the saturation of the process. The pattern leading to the saturation can be characterized through one specific dimensionless quantity called the Pierce parameter, which reads [7,19]

$$\rho = \frac{C_\rho}{\gamma}\left[J(\lambda_u K f_b(\xi))^2\right]^{1/3}, \quad C_\rho = 8.63 \times 10^{-3}$$

$$K = \frac{eB\lambda_u}{2\pi m_e c}, \quad f_b(\xi) = J_0(\xi) - J_1(\xi)$$

$$\xi = \frac{1}{4}\frac{K^2}{1 + \frac{K^2}{2}} \tag{12}$$

where J is the bunch current density, K is the strength parameter (another non-dimensional quantity), and the Bessel factor is a function of dimensionless quantities. The Pierce parameter ρ is a key quantity useful for specifying the growth rate, expressed through the gain length, defined as

$$L_g = \frac{\lambda_u}{4\pi\sqrt{3}\rho} \tag{13}$$

and the saturated power (P_S), expressed in terms of the electron beam power P_E as

$$P_F \simeq \sqrt{2}\rho P_E \tag{14}$$

The physical reasons, underlying Equation (17), can be traced back to a balance argument resembling that already mentioned in the case of the Renieri-limit. We note that:

(i)   The laser gain relative line width $\delta\omega_l/\omega_l$ is proportional to the Pierce parameter and to the maximum energy delivered from the e-beam to the laser field associated with the electron beam fractional energy variation. Therefore, we have

$$\frac{\Delta E_e}{E_e} \propto \frac{\delta\omega_l}{\omega_l} \propto \rho \tag{15}$$

(ii)   The electron beam power is

$$P_E = E_e I_e \tag{16}$$

where I_e is the e-beam current.

Hence, using Equations (15) and (16) yields

$$\Delta P_e \propto \rho P_e \tag{17}$$

and because, for conservation reasons, ΔP_e is the power delivered to the laser, we recover (separate an unessential numerical factor) Equation (16). A remarkable feature that comes out of the previous discussion is that, by defining the dimensionless length

$$\bar{z} = \frac{z}{L_g} \tag{18}$$

where z is the longitudinal coordinate along which the e-beam is progressing, it is possible to recover with a significant degree of accuracy the curve describing the growth of the laser field intensity from start up to saturation (see Figure 3) ([20,21] and the references therein)

$$P(\bar{z}) = P_0 \frac{A(\bar{z})}{1 + \frac{P_0}{P_F}[A(\bar{z}) - 1]} \tag{19}$$

$$A(\bar{z}) = \frac{1}{9}\left[3 + 2\cosh(\bar{z}) + 4\cos\left(\frac{\sqrt{3}\bar{z}}{2}\right)\cosh\left(\frac{\bar{z}}{2}\right)\right]$$

and also the evolution of the intensity induced electron bunch energy spread, namely

$$\sigma_i(\bar{z}) \simeq 3C_\sigma \sqrt{\frac{A(\bar{z})}{1 + 9B_\sigma[A(\bar{z}) - 1]}}$$

$$C_\sigma = \frac{1}{2}\sqrt{\frac{\rho_1 P_0}{P_E}}, \qquad B_\sigma \simeq \frac{1.24}{9}\frac{P_0}{P_F} \tag{20}$$

$$\sigma_{i,F} \simeq \frac{C_\sigma}{\sqrt{B_\sigma}} \simeq 1.6\rho$$

The physical meaning behind the previous equations is that the laser growth does not occur at the expense of only the electron energy, but also with a worsening of the beam qualities, which is the major element determining the saturation of the process. A larger energy spread means a reduction of the growth rate through an increase of the gain length. This can be accounted for in terms of dimensionless quantities too. It will be indeed sufficient to replace, in the definition of the gain length, the following expression

$$L_g \to \chi L_g$$

$$\chi = \left(1 + d_\chi \tilde{\mu}_\varepsilon^2\right), \quad d_\chi \simeq 0.185 \frac{\sqrt{3}}{2} \tag{21}$$

$$\tilde{\mu}_\varepsilon = 2\frac{\sigma_\varepsilon}{\rho}$$

with σ_ε being the RMS relative energy spread. The derivation of Equation (21) is the result of a joint effort, embedding theoretical considerations and fitting procedures (which have provided the determination of the numerical coefficient).

Accordingly a non-ideal energy spread determines the increase of the undulator length, that which is necessary to reach the saturation level. The relevant predictions yield indications for the impact of the quality of the beam on the cost of the whole device.
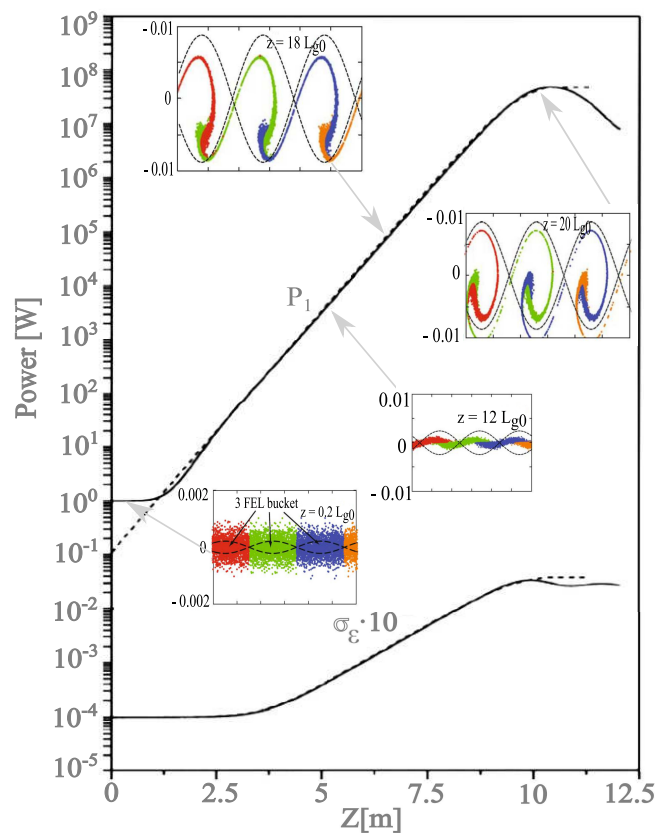

Figure 3. Growth of the FEL power and of the induced energy spread, as predicted by Equations (21) and (22) (dotted lines, continous numerical) along with the e-beam longitudinal phase modifications.

The minimal point of view on the design of complex devices, which we have thus far provided, will be further corroborated in the forthcoming section.

4. Instabilities in Tokamaks and Electron Accelerators

The growth of electromagnetic power in free electron coherent radiation generators is marked by the onset of a specific instability [22,23], whose evolution rate scales with the beam current raised to the characteristic exponent 1/3. Other instabilities (see below) affecting the e-beam in accelerating devices display growth rates exhibiting similar scaling [24–31]. When both FELs and other instabilities are active, their interplay has generated significant interest in the past [32]. Hot magnetic fusion plasmas are affected by different macroscopic instabilities which may hamper the relevant confinement. One of these is the sawtooth instability (STI) [33], which is characterized by periodic relaxations of the plasma

density and temperature. Typical effects of temperature and current density oscillation are reported in Figure 4. Using a purely phenomenological point of view, it is possible to conclude that such a behavior can be traced back to a nonlinear coupling between these quantities, governed by two equations [34,35] closely resembling the Volterra–Lotka prey–predator model [36,37], namely

$$
\begin{aligned}
\frac{dT_e}{dt} &= \nu_T T_e (1 - \alpha j) \\[2mm]
\frac{dj_e}{dt} &= -\nu_j j_e (1 - \beta T_e)
\end{aligned}
\tag{22}
$$

where T_e is the electronic plasma temperature and j is the current density. The constants $\nu_{T,j}$ are associated with the temperature rise time and current density damping time, respectively. The nonlinear coupling occurs through the coupling terms αj and βT_e. Without entering into the details of the physical mechanisms underlying plasma microwave instability, which can for example be found in [34], we simply mention that the temperature oscillations can be excited by an appropriate adjustment of the q-safety factor, by means of a co- and counter-Electron Cyclotron Current Drive (for further comments see [35]).

Regarding the FEL, it is worth stressing that it arises as an instability. Likewise, other instabilities affecting the beam may generate noise, which at macroscopic level determines the increase of the energy spread and bunch length. FELs and other instabilities may eventually give rise to a nonlinear competition.
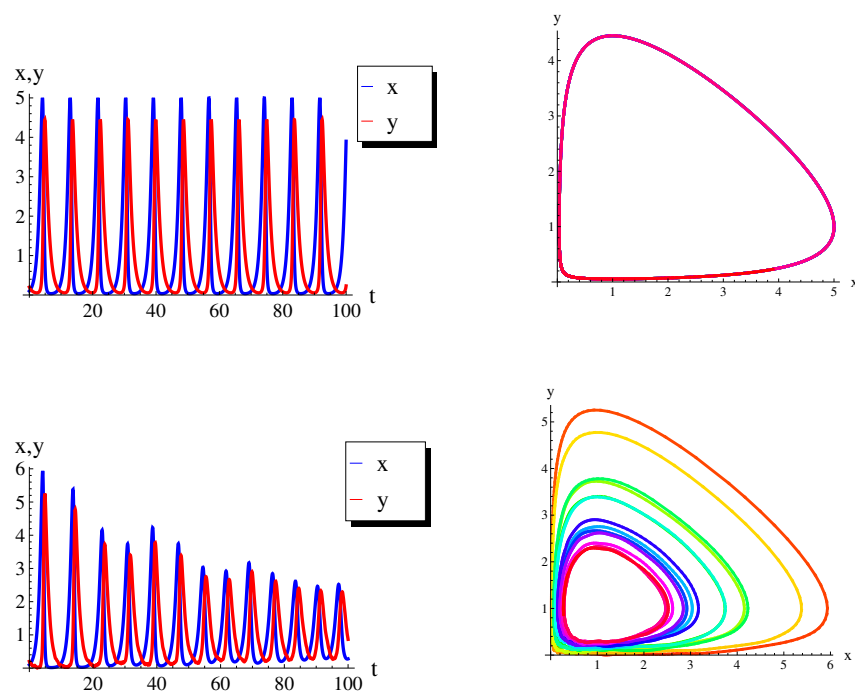

Figure 4. Top-Left: solution of Equation (24) with no noise; **Top-Right**: phase space of the dynamic variables x and y in the case of zero noise for the Lotka–Volterra equation system; **Bottom-Left**: solution of Equation (24) with the addition of white noise; **Bottom-Right**: phase space of the dynamic variables x and y in the case of white noise for the Lotka–Volterra equation system. Used parameters: $a = 1.1, c = 0.9, x(0) = 0.1, y(0) = 0.2$, noise amplitude = 0.2 (only for bottom plots, otherwise zero).

The competition is due to the feedback between the respectively induced disorders on the electron beam, which can lead to the collapse of one of the two growing instabilities. Empirical procedures based on white noise excitation in the radio frequency cavities of the SR have been used to partially "stabilize" and reduce the instabilities [23]. When

the electron beam passes many times within the interaction region, the process does not preserve any memory of the micro-bunch interaction correlated to the FEL, and the long time effect of the multi-turn interaction on the beam is that of a noisy contribution. Our analysis will be limited to the SR manifestation of the microwave instability [38,39], which appears as a fast blowup in the bunch length (or in the energy spread) followed by a damping, in SRs with an intense beam and a strong damping effect. The equations [32]

$$
\frac{d\bar{\sigma}^2}{dt} = \bar{\sigma}^2\left(\alpha - \frac{2}{\tau_s}\right)
$$

$$
\frac{d\alpha}{dt} = \alpha\left[\frac{A}{(1+\bar{\sigma}^2)^{1/4}} - B(1+\bar{\sigma}^2)^{1/2}\right]
$$

(23)

where A, B are constants expressed in terms of the SR characteristic parameters, describe the interplay between the evolution of the noise induced energy spread $\bar{\sigma}$ and the instability growth rate α. The previous equations can be cast exactly in a Lotka–Volterra form, for values of the induced energy spread not exceeding unity, we indeed find [40]

$$
\frac{dx}{dt} = ax(1-y)
$$
$$
\frac{dy}{dt} = -cy(1-x)
$$
$$
a = A - B, \quad c = \frac{2}{\tau_s}
$$
$$
x = \frac{\tau_s}{2}\alpha, \quad y = \frac{A+2B}{A-B}\frac{\bar{\sigma}^2}{4}
$$

(24)

The integration of the previous system of nonlinear equations yields the behavior reported in Figure 4, and an important result is that the inclusion of random noise, the part governing the evolution of the energy spread (or equivalently, the temperature T_e), determines the suppression of the instability itself. Either for plasma or SR sawtooth instabilities, the addition of noise, e.g. an external additional heating source, determines a reduction or even a suppression. In the case of the SR, it has been shown that the superposition of FEL induced energy spread may inhibit the insurgence of the instability, or on the contrary, a strong sawtooth may hamper the FEL operation. An additional example of instability is one emerging in accelerator physics and shares analogies in plasma physics, the so called micro-bunching instability [41], which arises when an e-bunch is compressed to increase its peak current and operate an X-ray FEL avoiding long undulators to reach the saturation. A crucial element to suppress this kind of instability is the so called laser heater device [42–47], designed to induce an energy spread to in turn reduce the instability growth rate, thus eventually determining further beam brightness dilution, which is harmful for FEL operation. The leitmotiv of the previous discussion is that the accelerator and plasma beams are affected by instabilities, which for at least for those of the microwave type, can be traced back to a common physical origin. The possible "cures" foresee the use of an external heater, although a more thorough analysis will be discussed elsewhere.

5. Conclusions

We have thus far mentioned the importance of feedback mechanisms in complex physical systems. These regulation mechanisms have profound roots in applied science (including the economy [48]), which can be traced back to fundamental concepts such as the Landau damping [49] and Le Chatelier's principle [50]. We should again mention their role in restoring the equilibrium symmetry or in creating the conditions for equilibrium. These topics are of central importance and will be the topic of a forthcoming investigation. The point we tried to convey in the last section is that the mechanisms underlying the growth and the regulation of the instability in the accelerator and fusion plasma can be, in principle, associated with mechanisms sharing some analogies, which then manifest

themselves into the behavior of certain macroscopic quantities. The consequences of the sawtooth on the SR e-beam is responsible for an increase in the energy spread and in the bunch length, which agree with the dilution of the beam brightness. Regarding the plasma temperature oscillations, they may determine confinement problems.

Furthermore, we have underscored that in FEL-SR devices, the growth of the laser field provides the necessary conditions (namely, an increase of noise determining the increase in the beam energy spread and decrease in the current density) to suppress the sawtooth itself. In a similar way, the injection of external heating sources induces an increase in the temperature responsible for the relaxation of the nonlinear oscillations.

Most interestingly, for practical purposes, the understanding of the underlying physics of the instability may provide suggestions for specific issues determining their "cures".

As already underscored, the use of an "external heater" has been of crucial importance in instability suppression for accelerators. Its physical roots, counteracting the underlying mechanism of the instability, trace back to important effects associated with the interplay between disorder and nonlinearity [22].

The practice of increasing the beam's lifetime in the storage ring by adding noise to the RF cavities has been used since the 1980s [23]. The use of a laser beam heater to counteract the micro-bunch instability has been commonly used in existing X-ray FEL devices [24–29]. Accordingly, the use of "external additional heating" to avoid instabilities became a common practice alongside magnetic fusion.

Regarding the design of FELs and Tokamaks as complex systems, we have envisaged the thread of a strategy starting from analogous conceptual tools, mainly based on the systematic use of easily manageable formulae, allowing the fixing of the device working point to be eventually benchmarked by a massive computation campaign. The examples we have exploited regarding the dimensioning of Tokamaks have been addressed with the goal of understanding the general criteria for embedding engineering quantities of different types, which are assembled to determine formulae useful for design purposes. In reality, the procedure is less straightforward. Much effort has been made in the past to reconcile the scaling relationship with theory. Although models predict local single phenomena, they fail in providing the global characteristics of the plasma confinement. Modeling and numerical analysis are important, but the empirical scaling relations inferred from statistical data and experiments play a major role. In this respect, the design of Tokamaks and FELs are different. In the last case, the agreement between theory, experiments, and scaling is fairly good. The same does not apply to plasma acceleration [51–53], which can exhibit significant differences between simulation, theory, and experiments. As concluding comment, we stress that the scaling formula [30] has become one of the crucial tools for ITER design.

Author Contributions: Conceptualization G.D. and E.D.P., writing—original draft preparation, G.D. and E.D.P.; writing—review and editing, A.C., G.D. and E.D.P.; visualization, A.C., G.D. and E.D.P. All authors have read and agreed to the published version of the manuscript.

Data Availability Statement: Not applicable.

Conflicts of Interest: The authors declare no conflicts of interest.

References

1.　Dattoli, G.; Palma, E.D.; Sabtchevsky, S.; Spassovsky, I. *High Frequency Sources of Coherent Radiation for Fusion Plasmas*; IOP Publishing: Bristol, UK, 2021.
2.　Colson, W.B.; Pellegrini, C.; Renieri, A. (Eds.) *Laser Handbook Vol. VI : Free Electron Lasers*; North Holland: Amsterdam, The Netherlands, 1990; ISBN-13 978-0444869531
3.　Wesson, J.; Campbell, D.J. *Tokamaks*; Clarendon Press: Oxford, UK, 2004.

4. Peeters, A.G. The Physics of Fusion Power, Lecture 2. Available online: https://warwick.ac.uk/fac/sci/physics/research/cfsa/people/pastmembers/peeters/teaching/lecture2.pdf (accessed on 8 May 2012).

5. Renieri, A. Storage ring operation of the free-electron laser: The amplifier. *Nuov. Cim. B* **1979**, *59*, 160–178. [CrossRef]

6. Dattoli, G.; Pellegrini, C. Riding The FEL Instability (Dedicated To Alberto Renieri). In Proceedings of the 39th International Free Electron Laser Conference (FEL2019), Hamburg, Germany, 26–30 August 2019. [CrossRef]

7. Dattoli, G.; Renieri, A.; Torre, A. *Lectures on Free Electron Laser Theory and Related Topics*; World Scientific: Singapore, 1993. [CrossRef]

8. Freidberg, J.P.; Mangiarotti, F.J.; Minervini, J. Designing a Plasma fusion reactor-How does a plasma fit in? *Phys. Plasmas* **2015**, *22*, 070901. [CrossRef]

9. Tsunematsu, T. The scaling law of energy confinement time for ITER. *Fusion Eng. Des.* **1991**, *15*, 309–310. [CrossRef]

10. Martin, Y.R.; Takizuka, T. Power requirement for accessing the H-mode in ITER. *J. Phys. Conf. Ser.* **2008**, *123*, 012033. [CrossRef]

11. Zohm, H. On the Use of High Magnetic Field in Reactor Grade Tokamaks. *J. Fusion Energy* **2019**, *38*, 3–10. [CrossRef]

12. Zohm, H. *Magnetohydrodynamic Stability of Tokamaks*; WILEY-VCH Verlag GmbH & Co. KGaA: Weinheim, Germany, 2015.

13. Zohm, H. On the size of tokamak fusion power plants. *Phil. Trans. R. Soc. A* **2019**, *377*, 20170437. [CrossRef]

14. Sarazin, Y.; Hillairet, J.; Duchateau, J.-L; Gaudimont, K.; Varennes, R.; Garbet, X.; Ghendrih, P.; Guirlet, R.; Pégourié, B.; Torre, A. Impact of scaling laws on tokamak reactor dimensioning. *Nucl. Fusion* **2019**, *60*, 016010. [CrossRef]

15. Costley, A.E.; Hugill, J.; Buxton, P.F. On the power and size of tokamak fusion pilot plants and reactors. *Nucl. Fusion* **2015**, *55*, 033001. [CrossRef]

16. Kadomtsev, B.B. Tokamaks and dimensional analysis. *Sov. J. Plasma Phys. (Engl. Transl.)* **1975**, *1*, 295–1975.

17. Calabrò, G.; Crisanti, F.; Ramogida, G.; Albanese, R.; Cardinali, A.; Cucchiaro, A.; Granucci, G.; Maddaluno, G.; Marinucci, M.; Nowak, S.; et al. FAST plasma scenarios and equilibrium configurations. *Nucl. Fusion* **2009**, *49*, 055002. [CrossRef]

18. Dattoli, G.; Di Palma, E.; Sabia, E. Is there anything new to say about dimensions in Physics. *Growth Form* **2022**, *3*, 3–22. [CrossRef]

19. Colson, W.B. Theory of high gain Free Electron Lasers. *Nucl. Instruments Methods Phys. Res. A* **1997**, *393*, 82–85. [CrossRef]

20. Dattoli, G.; Ottaviani, P.L. Semi-analytical models of free electron laser saturation. *Opt. Commun.* **2002**, *204*, 283–297. [CrossRef]

21. Dattoli, G.; Di Palma, E.; Licciardi, S.; Sabia, E. Free Electron Laser High Gain Equation and Harmonic Generation. *Appl. Sci.* **2021**, *11*, 85. [CrossRef]

22. Bishop, A.R.; Campbell, D.K.; Pnevmatikos, S. (Eds.) *Disorder and Nonlinearity: Proceedings of the Workshop JR Oppenheimer Study Center Los Alamos, New Mexico, 4–6 May, 1988*; Springer Science Business Media: Berlin, Germany, 2012; Volume 39.

23. Sakanaka, S.; Izawa, M.; Mitsuhashi, T.; Takahashi, T. Improvement in the beam lifetime by means of an rf phase modulation at the KEK Photon Factory storage ring. *Phys. Rev. Spec.-Top.-Accel. Beams* **2000**, *3*, 050701. [CrossRef]

24. Saldin, E.; Schneidmiller, E.; Yurkov, M. Klystron instability of a relativistic electron beam in a bunch compressor. *Nucl. Inst. Methods A* **2002**, *490*, 1–8. [CrossRef]

25. Heifets, S.; Stupakov, G.; Krinsky, S. Coherent synchrotron radiation instability in a bunch compressor. *Phys. Rev. ST AB* **2002**, *5*, 064401. [CrossRef]

26. Saldin, E.; Schneidmiller, E.; Yurkov, M. Longitudinal space charge driven microbunching instability in the TESLA Test Facility Linac. *Nucl. Inst. Methods A* **2004**, *528*, 355. [CrossRef]

27. Huang, Z.; Borl, M.; Emma, P.; Wu, J.; Limborg, C.; Stupakov, G.; Welch, J. Suppression of microbunching instability in the linac coherent light source. *Phys. Rev. ST AB* **2004**, *7*, 074401.

28. Wu, J. *Temporal Profile of the LCLS Photocathode Ultraviolet Drive Laser Tolerated by the Microbunching Instability*; SLAC-PUB-10430; SLAC National Accelerator Lab.: Menlo Park, CA, USA, 2004.

29. Angelova, G.; Ziemann, V.; Meseck, A.; Hamberg, B.M.; Salén, P.; Van Der Meulen, P.; Winter, A. Installation of the Optical Replica Synthesizer in FLASH. In Proceedings of the the 29th Free Electron Laser Conference FEL07, Novosibirsk, Russia, 26–31 August 2007.

30. Uckan, N.A. *ITER Physics Guidelines*; International Atomic Energy Agency: Vienna, Austria, 1989.

31. ITER Physics Expert Group on Confinement and Transport. Plasma confinement and transport. *Nucl. Fusion* **1999**, *39*, 2175–2249. [CrossRef]

32. Bartolini, R.; Dattoli, G.; Mezi, L.; Renieri, A.; Migliorati, M.; Couprie, M.E.; De Ninno, G.; Roux, R. Suppression of the Sawtooth Instability in a Storage Ring by Free-Electron Laser: An Example of Nonlinear Stabilization by Noise. *Phys. Rev. Lett.* **2001**, *87*, 134801. [CrossRef]

33. Hastie, R.J. Sawtooth Instability in Tokamak Plasmas. *Astrophys. Space Sci.* **1977**, *256*, 177–204. [CrossRef]

34. Giruzzi, G.; Imbeaux, F.; Ségui, J.L.; Garbet, X.; Huysmans, G.; Artaud, J.F.; Bécoulet, A.; Hoang, G.T.; Litaudon, X.; Maget, P.; et al. New Tokamak Plasma Regime with Stationary Temperature Oscillations *Phys. Rev. Lett.* **2003**, *91*, 135001. [CrossRef]

35. Turco, F.; Giruzzi, G.; Imbeaux, F.; Udintsev, V.S.; Artaud, J.F.; Barana, O.; Dumont, R.; Mazon, D.; Ségui, J.-L. O-regime dynamics and modeling in Tore Supra, *Phys. Plasmas* **2009**, *16*, 062301. [CrossRef]

36. Lotka, A.J. Undamped oscillations derived from the law of mass action. *J. Am. Chem. Soc.* **1920**, *42*, 1595–1599. [CrossRef]

37. Volterra, V. Fluctuations in the Abundance of a Species considered Mathematically. *Nature* **1926**, *118*, 558–560. [CrossRef]

38. Krejcik, P.; Bane, K.; Corredoura, P.L.; Decker, F.J.; Judkins, J.; Limberg, T.; Minty, G.; Siemann, R.H.; Pedersen, F. High intensity bunch length instabilities in the SLC damping rings. In Proceedings of the 15th IEEE Particle Accelerator Conference, Washington, DC, USA, 17–20 May 1993; pp. 3240–3242.

39. Laclare, J.L. Introduction to Coherent Instabilities-Coasting Beam Case. *CAS CERN Accel. Sch. Gen. Accel. Phys.* **1984**, 377–414. [CrossRef]

40. Migliorati, M.; Palumbo, L.; Dattoli, G.; Mezi, L. A Sawtooth Instability in Storage Rings. In Proceedings of the 1999 Particle Accelerator Conference, New York, NY, USA, 28 May–3 June 1999; pp. 1219–1221.

41. Alcaraz, J.; Alpat, B.; Ambrosi, G.; Azzarello, P.; Battiston, R.; Bertucci, B.; Bolmont, J.; Bourquin, M.; Burger, W.J.; Capell, M.; et al. The alpha magnetic spectrometer silicon tracker: Performance results with protons and helium nuclei. *Nucl. Instrum. Methods Phys. Res. Sect. Accel. Spectrometers Detect. Assoc. Equip.* **2008**, *593*, 376–398. [CrossRef]

42. Spampinati, S.; Di Mitri, S.; Diviacco, B. Modeling of a Laser Heater for Fermi@Elettra. In Proceedings of the FEL 2007 Conference, Novosibirsk, Russia, 26–31 August 2007; pp. 362–365.

43. Angelova, G.; Ziemann, V.; Meseck, A.; Salén, P.; van der Meulen, P.; Hamberg, M.; Larsson, M.; Bödewadt, J.; Khan, S.; Winter, A.; et al. Results from the optical replica experiment in FLASH. In Proceedings of the European Particle Accelerator Conference, Genoa, Italy, 23–27 June 2008; pp. 2695–2697.

44. Emma, P. First Lasing of the LCLS X-Ray FEL at 1.5 Å. In Proceedings of the Particle Accelerator Conference (PAC 09), Vancouver, QC, Canada, 4–8 May 2009; p. TH3PBI01.

45. Dattoli, G.; Migliorati, M. A model of laser heater undulator system for self-amplified free electron lasers. *J. Appl. Phys.* **2009**, *105*, 023111. [CrossRef]

46. Nuhn, H.-D. *Linac Coherent Light Source (LCLS) Conceptual Design Report*; Report SLAC-R-593; Stanford Linear Accelerator Center, Stanford University: Stanford, CA, USA, 2002. [CrossRef]

47. Dattoli, G.; Labat, M.; Migliorati, M.; Ottaviani, P.L.; Pagnutti, S.; Sabia, E. The FEL SASE operation, bunch compression and the beam heater. *Opt. Commun.* **2011**, *284*, 1945–1950. [CrossRef]

48. Kusumoto, S.I. Extensions of the Le Chatelier-Samuelson Principle and Their Application to Analytical Economics–Constraints and Economic Analysis. *Econom. J. Econom. Soc.* **1976**, *44*, 509–535. [CrossRef]

49. Landau, L.D. *Collected Papers of LD Landau*; Elsevier: Amsterdam, The Netherlands, 1965.

50. Chatelier, H.L. On a general statement of the laws of chemical equilibrium. *C. R.* **1884**, *99*, 786–789.

51. Tajima, T.; Dawson, J.M. Laser electron accelerator. *Phys. Rev. Lett.* **1979**, *43*, 267. [CrossRef]

52. Malka, V.; Faure, J.; Gauduel, Y.A.; Lefebvre, E.; Rousse, A.; Phuoc, K.T. Principles and applications of compact laser—Plasma accelerators. *Nat. Phys.* **2008**, *4*, 447–453. [CrossRef]

53. Esarey, E.; Schroeder, C.B.; Leemans, W.P. Physics of laser-driven plasma-based electron accelerators. *Rev. Mod. Phys.* **2009**, *81*, 1229. [CrossRef]